Harmonic Compensation with Active Loads Designed for Power Quality Improvement in Microgrids

Ioan Serban, *Member, IEEE*
Department of Electrical Engineering and Applied Physics
Transilvania University of Brasov
Brasov, Romania
ioan.serban@unitbv.ro

***Abstract*— Ensuring a proper power quality level in microgrids (MGs) represents a major challenge and requires exploiting most of the MG available resources. An important measure consists in modifying the interaction of conventional consumers with the MG, thereby aiming to the development of active loads (ALs). Besides voltage and frequency support, an AL can provide harmonic compensation (HC) according to its operational limits. Therefore, this paper presents a solution for HC, targeted to a particular class of ALs based on non-critical resistive loads. The main advantage of the proposed solution consists in the control method that enables HC to an AL with a minimalist structure of the power converter. The control method is validated by experimental results.**

Keywords*— microgrid; active load; harmonic compensation; smart grid;

I. INTRODUCTION

The development of the future smart grids based on interconnected microgrids (MGs) involves high technological advancements in order to ensure the system robustness, stability and power quality in systems with high penetration levels of distributed generators (DGs) based on renewable energy sources (RESs). For this purpose, besides the advanced support the generators can provide, the MG successful implementation highly depends of a better control at the consumption level, along with other specific resources such as energy storage systems. On this line, the active loads (ALs) - also termed as smart/flexible loads -, bring the advantages of better controllability, predictability and grid interaction features, such as voltage and frequency control. A particular category is represented by the smart appliances, which – along with electric vehicles – can be integrated into the smart grid infrastructure to perform demand response control [1], [2].

The ALs are commonly used for controlling the frequency in MGs during normal operational modes, or to prevent blackouts (e.g. in the load shedding mechanism) [3]-[6]. One particular smart load technology is the electric spring (ES). The ES is composed of a power electronic converter connected to a non-critical load. It can provide numerous ancillary services in grids [7] or MGs [8]-[12], such as voltage and frequency support, power factor correction, unbalances compensation. Due to the ES operational flexibility, a new function allowing compensating the harmonics have been recently developed [13], [14]. However, an ES requires a full bridge inverter and a complex control system, which are not always justified. Therefore, this paper suggests an HC control method for a particular class of ALs based on non-critical resistive loads, as introduced in [15]. Although the range of auxiliary functions provided is less than of an ES, the main advantage of the proposed solution over an ES consists in the reduced complexity of the power converter, in terms of both hardware topology and control. In terms of practicality, domestic water and space heating loads are most likely to become ALs, since short variations in their power consumption are generally not detrimental for the primary consumer. Therefore, an important opportunity for adding HC as an ancillary function becomes of interest for this type of loads.

An important point worth noting is that the proposed HC for ALs represents a feature similar to that of the inverters that interface RES generators, but which can also provide ancillary services such as harmonic compensation depending on its reserve capacity [16]-[18]. Therefore, through exploitation of various resources available in the MG, the negative effects produced by the non-linear loads can thus be mitigated.

II. PROPOSED AL CONTROL APPROACH

As mentioned in the preceding section, the targeted AL is based on non-critical resistive loads, which are usually found in electric space/water heating equipments. Therefore, the AL structure is optimally adapted for this type of resistive loads. Fig. 1 shows the typical integration of an AL within a consumer, which may also contain critical loads, where the system can be connected to the grid, or to an MG. In order to assess how the proposed control method can improve the local power quality, the critical load is considered being non-linear – which is a common case for residential consumers.

A. Control Principle

As shown in Fig. 1, the AL consists of a non-critical resistive load and a power electronic interface, which controls the power flow between the grid and the load. Regarding the power interface configuration, Fig. 2 presents two possible options, a single-switch AC/DC buck-converter (Fig. 2a) and an AC/AC buck converter (Fig. 2b). In both cases the power transferred to the load can be controlled by regulating the

978-1-5386-1495-2/18/$31.00 ©2018 IEEE

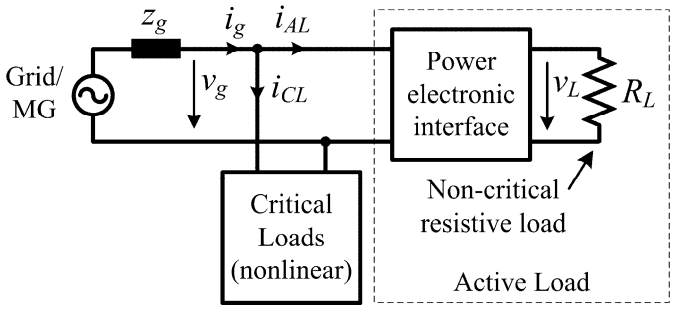

Fig. 1. AL structure and typical use in combination with a critical load

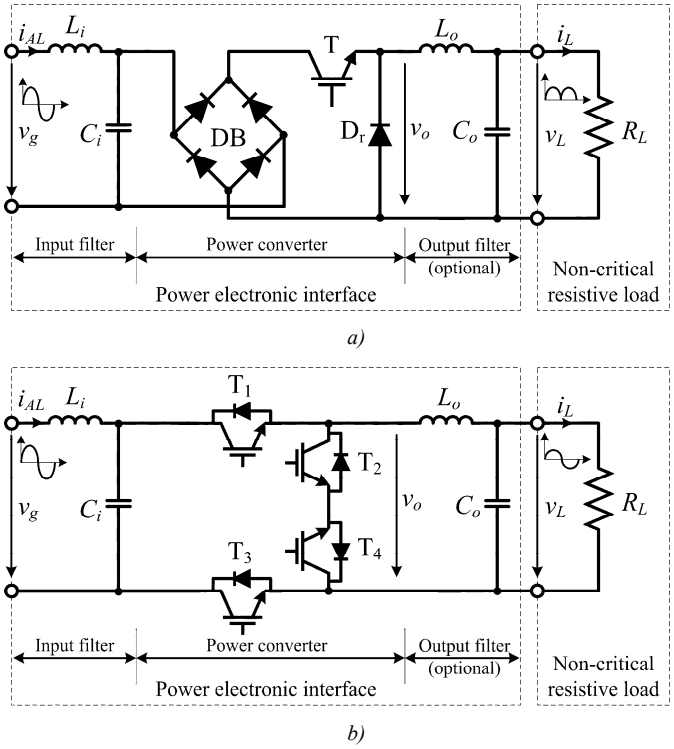

Fig. 2. Targeted AL configurations: a) Single-switch AC/DC buck converter; b) AC/AC buck converter

output voltage v_L. Each configuration has three main components, namely the input filter, a power converter and an optional output filter. The input filter is included to attenuate the high-frequency current ripple, while the output filter can be added to improve the output voltage shape by removing the high-frequency voltage components. However, if the non-critical load can be supplied directly with the PWM voltage produced by the converter (v_o), the AL complexity can be reduced by removing the output filter. Therefore, the hereinafter analysis is considered for the case without the output filter.

The main difference between the two topologies shown in Fig. 2 consists in the shape of the voltage they produce at the output, namely the converter from Fig. 2a generates a unipolar output voltage, while the other one (Fig. 2b) produces a bipolar AC voltage. However, as the concerned loads (i.e., thermal resistive loads) are generally not influenced by the voltage shape and polarity, the AL structure from Fig. 2a is of more interest due to its lower hardware complexity in comparison with the AC-AC buck topology from Fig. 2b.

For both AL configurations presented in Fig. 2, the RMS output voltage (V_L) can be controlled, as expressed in (1), by means of a constant duty cycle (D_0), used to generate either a single PWM signal for the transistor T from Fig. 2a [6] or four PWM signals for the topology from Fig. 2b [19]. If the output filter is removed, as previously mentioned, the RMS output voltage will be expressed by (1a), while in the case with output filter designed to mitigate most of the high-frequency components (i.e., the output voltage v_L is sinusoidal) the correct form of the RMS output voltage is provided by (1b). Certainly, the load resistor R_L is assumed quasi-ideal, neglecting its self-inductance. Therefore, considering the case with no output filter (as previously mentioned), while neglecting the voltage drops on the converter components, the AL input power will become directly proportional with D_0, as expressed in (2). It should also be mentioned that, since the conventional control of such converters has been presented in the literature, this paper will focus only on the new control approach that enables the AL to provide HC.

Due to the relatively high switching frequency of the PWM signal, a considerable control bandwidth of the AL input current (i_{AL}) can be achieved. Therefore, besides controlling the fundamental current component, the AL can also generate harmonics within a certain spectrum. By exploiting this feature, this paper proposes enhancing the AL control with HC, this way improving the power quality in systems with nonlinear loads.

$$V_L = V_g\sqrt{D_0} \tag{1a}$$

$$V_L^{'} = V_g D_0 \tag{1b}$$

$$P_L = \frac{V_g^2}{R_L} D_0 \tag{2}$$

Neglecting the voltage drop on the inductor L_i, the input current can be expressed as in (3), where, in the conventional control approach, $D(t)$ is the duty cycle D_0 from (1a) and (2), which remains constant in a period of the input voltage. By this way, assuming the input voltage v_g sinusoidal, the AL current i_{AL} will contain only the fundamental component.

$$i_{AL}(t) = \frac{v_g(t)}{R_L} D(t) \tag{3}$$

The implementation of the proposed idea involves adding variable components ($D_H(t)$) to the average duty cycle D_0, with the main purpose of generating current harmonics, as follows:

$$D(t) = D_0 + D_H(t) \tag{4}$$

$$D_H(t) = \sum_{h=3,5,7,9} D_{h-1} \sin\left[(h-1)\omega t + \varphi_{h-1}\right] \tag{5}$$

With the new expression of *D(t)* provided in (4)-(5), the AL current can be determined from (6), where, besides the fundamental component (i_{AL1}), the main odd harmonic components (i.e., h=3,5,7,9) can also be produced as expressed in (7). In order to produce the h^{th} current harmonic, the amplitude and phase of both side components of the duty cycle must be controlled (i.e., $D_{h\pm1}$ and $\varphi_{h\pm1}$), as expressed in (8)-(9). Because of the coupling between a certain current harmonic and its side duty cycle components, a change of the h^{th}–order duty cycle affects all current harmonics. Therefore, the algorithm that controls the HC has to recalculate all duty cycles each time one harmonic of the input current is changed. However, by targeting only the main harmonics components (i.e., 3rd to 9th), a simplification of the control algorithm is ensured. Therefore, considering h_{max}=9, expression (10) provides the values for the upper duty cycle component, which can be then used to calculate all the other harmonic components using (8)-(9).

Another point worth noting is that, since the duty cycle is confined between 0 - 1, the harmonic component D_H must be limited within the duty cycle reserve, which depends on the average value (D_0), as described in the next subsection.

$$i_{AL}(t) = i_{AL1}(t) + i_{ALh}(t) \tag{6}$$

$$i_{ALh}(t) = \sum_{h=3,5,7,9} I_{ALh} \sin\left(h\omega t + \delta_{ALh}\right) \tag{7}$$

$$D_{h-1} = \sqrt{D_{h+1}^2 + \frac{4R_L^2}{V_g^2} I_{ALh}^2 + \frac{4R_L}{V_g} I_{ALh} D_{h+1} \sin\left(\varphi_{h+1} - \delta_{ALh}\right)} \tag{8}$$

$$\varphi_{h-1} = atg\left[\frac{V_g D_{h+1} \cos\varphi_{h+1} - 2R_L I_{ALh} \sin\delta_{ALh}}{-V_g D_{h+1} \sin\varphi_{h+1} - 2R_L I_{ALh} \cos\delta_{ALh}}\right] - \frac{\pi}{2} \tag{9}$$

$$D_{h-1} = 2R_L I_{ALh} / V_g; \quad \varphi_{h-1} = \delta_{ALh} - \pi/2 \tag{10}$$

B. Proposed control system with enhanced HC feature

Fig. 3 shows the control scheme developed to ensure HC with the proposed AL. The HC loop is based on a proportional-resonant (PR) controller, expressed in (11) with k_{Hp} and k_{Hi} being the proportional and integral (resonant) gains. The controller provides the current reference i_{ALh}^* by selectively amplifying the harmonics to be compensated by the AL. Furthermore, a digital Fourier transform (DFT) is used to extract the magnitude (I_{ALh}) and phase (δ_{ALh}) of the harmonics to be controlled, which are then introduced into a block that calculates the required duty cycles (D_H) according to the equations described in the subsection A.

In order to control the component D_0 of the duty cycle from (4), which is associated with the fundamental current component, a current controller is developed according to the diagram presented in Fig. 4. By this control scheme the main function of the AL is ensured, namely to control the input active power (P_{AL}) according to the primary load requirements and the specific service the AL provides to the grid or MG (e.g., frequency support [15], [20]). The value of D_0 results as a sum between a feed-forward term (D_{FF}) - calculated from the active power reference (P_{AL}^*) and the grid voltage (V_g^*) according to (2) - , and a compensation term (D_c). In the compensation loop, a current controller based on a proportional-integrative (PI) structure is included to ensure an accurate tracking of the active current reference I_{ga}^*.

As previously mentioned, the HC capability is limited by the duty cycle reserve, which depends on the value of D_0. Obviously, when D_0 is at minimum or at maximum, there is no reserve left for harmonic generation, while the most advantageous situation for HC occurs at $D_0 = 0.5$. An important point worth mentioning here is that the HC limitation is similar to the case of DGs providing HC as an auxiliary service within the inverter remaining capacity. Therefore, in case of HC limitation, a selective (prioritized) harmonic generation algorithm is activated. Since the lowest order harmonics are usually the most harmful in a power system, in the current paper the developed algorithm is based on prioritizing the harmonics to be compensated inversely with their order (i.e. the 3rd–order is the first compensated harmonic). Nevertheless, any other selective technique can be implemented, according to the specific requirements of applications.

$$G_{PR}(s) = k_{Hp} + \frac{2k_{Hi}s}{s^2 + (h\omega_0)^2} \tag{11}$$

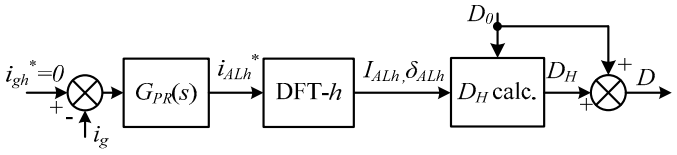

Fig. 3. AL HC control scheme.

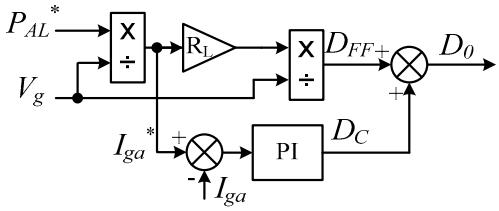

Fig. 4. AL fundamental current control scheme

III. Experimental Validation

The proposed HC control is assessed using a laboratory system implemented according to the scheme presented in Fig. 5. A 3kW AL is connected in parallel with a 0.5kW nonlinear load (single-phase diode rectifier with capacitive output filter), as part of the critical load. A constant-power mode control is imposed for the nonlinear load so that the input active power remains constant throughout the experiments. The AL PWM switching frequency is 15 kHz and the parameters of the input filter are as follows: L_i=400μH; C_i=10μF. The system is connected to a 230V/50Hz grid by means of an impedance of $Z_g = 0.4+j0.55\Omega$. On the control side, a dSPACE DS1103 board is employed to implement the control schemes presented in the previous section.

The HC is highlighted by comparing the response of the proposed AL with the conventional operating case (i.e. without HC). As Fig. 6 shows, without HC (Fig. 6a) the grid current (i_g) becomes highly distorted because of the non-linear characteristic of the load. In this case, the AL duty cycle is maintained constant to around 0.5, which corresponds to a reference power of P_{AL}^*=1.5kW. After the HC control is enabled, Fig. 6b shows that the grid current distortion decreases to less than 3%. As can be seen, the AL duty cycle includes a variable component (D_H from Fig. 3) superimposed over the average value D_0. Therefore, the AL input current (i_{AL}) is modified to compensate for the nonlinear currents produced by the critical load.

The AL capability to compensate the harmonics was also analyzed by changing the active power reference P_{AL}^* in between zero and rated value. Fig. 7 shows the variation of total harmonic distortion (THD) for the grid current according to P_{AL} for two cases, namely with and without HC. As can be seen, enabling the HC leads to a substantial improvement of the current distortions. In the optimal case (i.e. around half the output power, corresponding to $D_0 \cong 0.5$), the THD of the grid current is maintained under 3%, in contrast to the case without HC where the THD is almost ten times higher. However, as the output power reaches one of the extremities, the HC effectiveness decreases because of the HC limitation effect

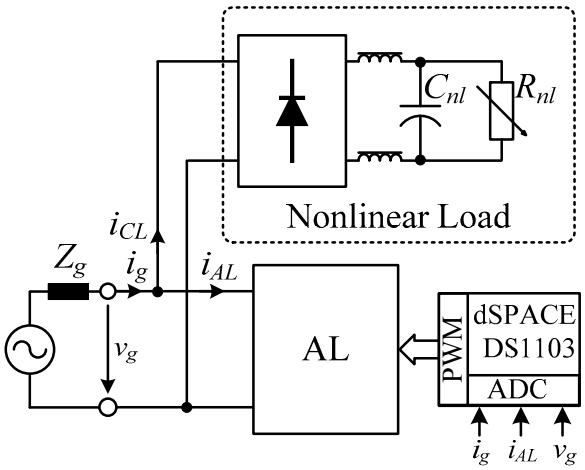

Fig. 5. Block diagram of the laboratory setup

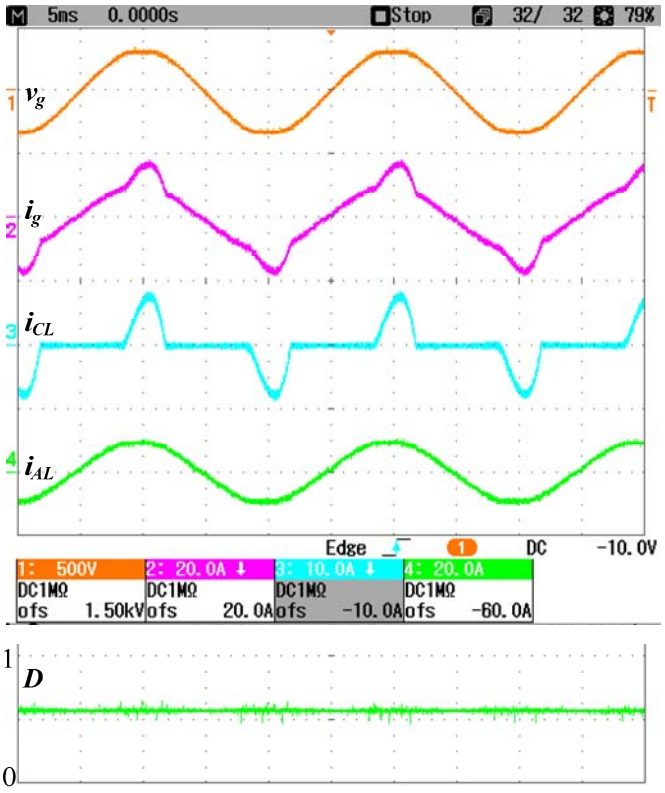

a)

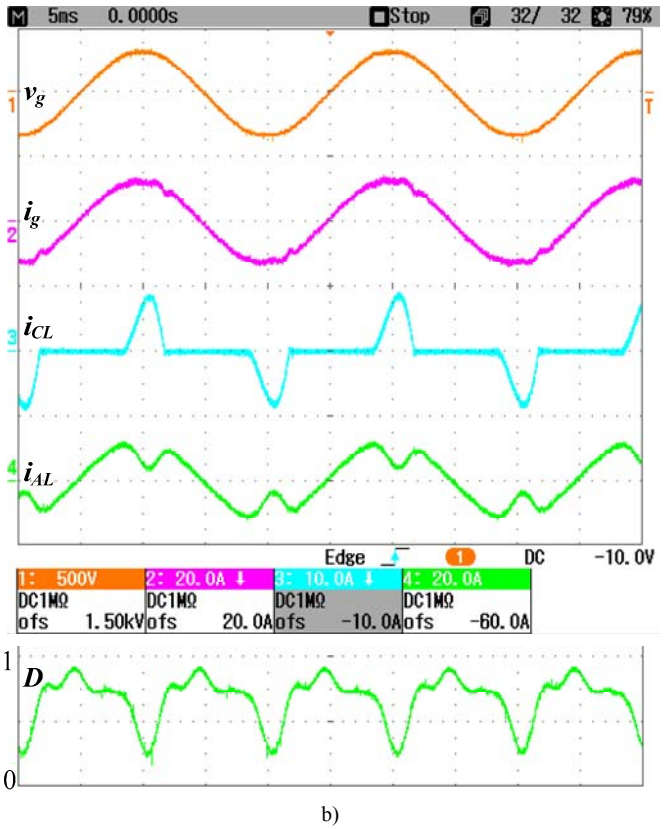

b)

Fig. 6. Experimental results (grid voltage v_g, grid current i_g, CL current i_{CL}, AL current i_{AL} and AL duty cycle D): a) without HC; b) with HC.

described in the previous section. In these conditions, the THD of grid current is limited to 5% for P_{AL} = 1…1.9kW.

As described in the previous section, whenever compensating all current harmonics is restricted by the AL operating conditions, a selective HC algorithm decides which components to be compensated. Therefore, a prioritization is carried out implying that the lowest order harmonics are compensated first. This functionality is demonstrated by the results included in Fig. 8, where each current harmonic between 3rd to 9th orders is represented in percent of the fundamental current according to the AL loading, with and without HC. As can be seen, all four harmonics are compensated properly when P_{AL} is around 1.5kW (i.e., $D_0 \cong 0.5$), which is the optimal operating case from the HC perspective. After exceeding this point, the THD slowly increases up to the value corresponding to the case without HC. Notice that, being assigned the highest priority in the HC algorithm, the 3rd order harmonic has the widest compensation interval, while the remaining harmonics are compensated within the reserve of the duty cycle. Fig. 8 also shows that, within the interval P_{AL} = 200-800W the 7th and 9th harmonics exhibit slightly higher values with HC than in the opposite case, the difference being no more than 1.5%. The effect is caused mainly by the operation conditions of the single-phase rectifier, which draws slightly more current harmonics as the input voltage becomes less distorted due to the AL compensating the lower-order harmonics (especially the 3rd order). However, when the duty cycle value allows compensating higher-order harmonics too, a significant reduction of the aforementioned harmonics can be noticed.

IV. Conclusions

A harmonic compensation (HC) control method applied to a certain class of active loads (ALs) based on non-critical resistive loads has been proposed in this paper. The main contribution of this study consists in the control method that allows the HC function to be applied to an AL having a minimalist power converter structure. The experimental results have shown that, in the presence of a nonlinear load, the grid current distortion can be significantly reduced with the proposed AL control method. In the AL optimal operating point, the grid current total harmonic distortion (THD) has been reduced from 22% in the case without HC to less than 3% after the AL HC was enabled. Furthermore, the paper has also revealed the AL HC capability greatly depends on the AL power loading. Therefore, for the cases when the compensation cannot be fully performed a selective harmonic generation algorithm based on harmonics order prioritization has been developed (in this paper the lowest order harmonic was associated with the highest compensation priority). The experimental results also have shown that the HC capability is maintained for the whole AL power range, it becoming less effective as the active power reaches one of the two extremities.

Acknowledgment

This work was supported by a grant of the Romanian National Authority for Research and Innovation, CCCDI UEFISCDI, project number ERANET LAC Call ELAC2015/T10-0761, RETRACT, within PNCDI III.

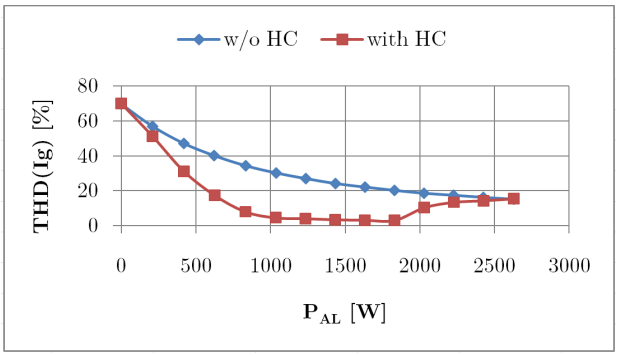

Fig. 7. Grid current THD according to AL loading, with and without HC.

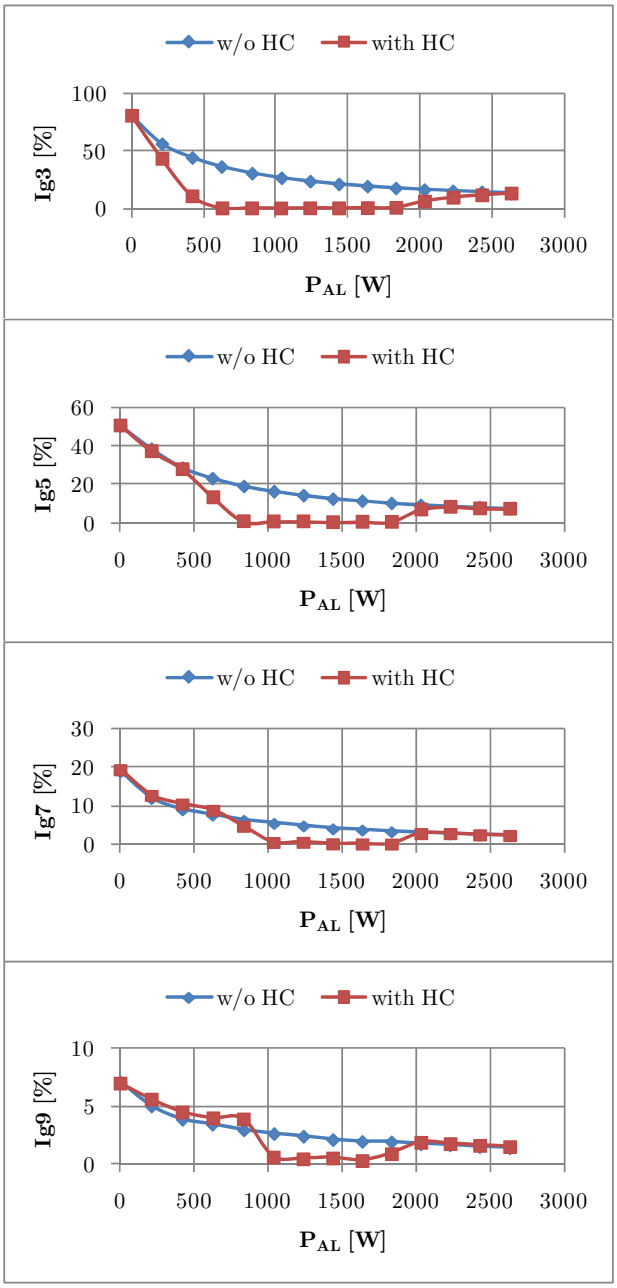

Fig. 8. Grid current harmonic content (3rd to 9th order) according to AL loading, with and without HC.

REFERENCES

[1] M. H. K. Tushar, C. Assi, M. Maier and M. F. Uddin, "Smart Microgrids: Optimal Joint Scheduling for Electric Vehicles and Home Appliances", IEEE Trans. Smart Grid, vol. 5, no. 1, pp. 239-250, Jan. 2014.

[2] P. Palensky and D. Dietrich, "Demand Side Management: Demand Response, Intelligent Energy Systems, and Smart Loads", IEEE Trans. Industrial Informatics, vol. 7, no. 3, pp. 381-388, Aug. 2011.

[3] A. Mondal, M.S. Illindala, A.S. Khalsa, D.A. Klapp, J.H. Eto, "Design and Operation of Smart Loads to Prevent Stalling in a Microgrid", IEEE Trans. Ind. Appl., vol. 52, no. 2, pp. 1184-1192, March-April 2016.

[4] R. Sebastián, "Application of a battery energy storage for frequency regulation and peak shaving in a wind diesel power system", IET Gener. Transm. Distrib., vol. 10, no. 3, pp. 764-770, March 2016.

[5] G. Ding, S. Zhang, J. Shan, F. Gao, X. Gu, "Autonomous control of active power electronics loads for frequency control of islanded microgrid," 2017 IEEE Energy Conversion Congress and Exposition (ECCE), Cincinnati, OH, 2017, pp. 1582-1587.

[6] I. Serban, C., Marinescu, "Aggregate load-frequency control of a wind-hydro autonomous microgrid", Renew. Energ., vol. 36, no. 12, pp. 3345-3354, Dec. 2011.

[7] Shu Yuen Hui, Chi Kwan Lee, F.F. Wu, "Electric Springs—A New Smart Grid Technology", IEEE Trans. Smart Grid, vol.3, no.3, pp.1552-1561, Sept. 2012.

[8] X. Chen, Y. Hou, S.C. Tan, C.K. Lee, S.Y.R. Hui, "Mitigating Voltage and Frequency Fluctuation in Microgrids Using Electric Springs", IEEE Trans. Smart Grid, vol. 6, no. 2, pp. 508-515, March 2015.

[9] Q. Wang, M. Cheng, Yunlei Jiang, Fujin Deng, Z. Chen and G. Buja, "Control of three-phase electric springs used in microgrids under ideal and non-ideal conditions", 42nd Annual Conference of the IEEE Industrial Electronics Society (IECON), Florence, 2016, pp. 2247-2252.

[10] S. Yan, M. h. Wang, T. b. Yang and S. Y. R. Hui, "Instantaneous frequency regulation of microgrids via power shedding of smart load and power limiting of renewable generation", IEEE Energy Conversion Congress and Exposition (ECCE), Milwaukee, WI, 2016, pp. 1-6.

[11] T. Yang, K. T. Mok, S. C. Tan, C. K. Lee, S. Y. R. Hui, "Electric Springs with Coordinated Battery Management for Reducing Voltage and Frequency Fluctuations in Microgrids", IEEE Trans. Smart Grid, in press.

[12] X. Chen, Y. Hou, S. Y. R. Hui, "Distributed Control of Multiple Electric Springs for Voltage Control in Microgrid", IEEE Trans. Smart Grid, vol. 8, no. 3, pp. 1350-1359, May 2017.

[13] Q. Wang, M. Cheng, Y. Jiang, "Harmonics Suppression for Critical Loads Using Electric Springs With Current-Source Inverters", IEEE J. Emerging Sel. Top. Power Electron., vol. 4, no. 4, pp. 1362-1369, Dec. 2016.

[14] S. Yan, S. C. Tan, C. K. Lee, B. Chaudhuri, S. Y. R. Hui, "Use of Smart Loads for Power Quality Improvement", IEEE J. Emerging Sel. Top. Power Electron, vol. 5, no. 1, pp. 504-512, March 2017.

[15] I. Serban, "Active Load Control for Dynamic Frequency Support and Harmonic Compensation in Autonomous Microgrids", ASCE's Journal of Energy Engineering, vol. 144, no. 2, Apr. 2018.

[16] Munir, S., and Li, Y.W., (2013). "Residential Distribution System Harmonic Compensation Using PV Interfacing Inverter", IEEE Trans. Smart Grid, vol. 4, no. 2, pp. 816-827, June 2013.

[17] R. Chilipi, N. Al Sayari, K. Al Hosani and A. R. Beig, "Control scheme for grid-tied distributed generation inverter under unbalanced and distorted utility conditions with power quality ancillary services", IET Renewable Power Generation, vol. 10, no. 2, pp. 140-149, 2 2016.

[18] T. Geury, S. Pinto and J. Gyselinck, "Current source inverter-based photovoltaic system with enhanced active filtering functionalities", IET Power Electronics, vol. 8, no. 12, pp. 2483-2491, 12 2015.

[19] T.B. Soeiro, C.A. Petry, J.C.d.S. Fagundes, I. Barbi, "Direct AC–AC Converters Using Commercial Power Modules Applied to Voltage Restorers", IEEE Trans. Ind. Electron., vol. 58, no. 1, pp. 278-288, Jan. 2011.

[20] I. Serban, C. P. Ion, "Supporting the dynamic frequency response in microgrids by means of active loads", 42nd Annual Conference of the IEEE Industrial Electronics Society (IECON), Florence, 2016, pp. 3781-3786.